Electronic Supporting Information

Symmetry control and magnetic exchange coupling in SMMs based on Co(II) complexes

Laura Cuevas-Contreras,[a] *María Mar Quesada-Moreno,*[b] *Estibaliz Ruiz-Bilbao,*[c] *Juan Manuel Gutiérrez-Zorrilla,*[c] *J. Krzystek,*[d] *Mykhaylo Ozerov,*[d] *Juan Ramón Jiménez,* [a,*] *Enrique Colacio*[a,*]

[a] Departamento de Química Inorgánica, Facultad de Ciencias, Universidad de Granada, 18071 Granada, Spain.

[b] Departamento de Química Física y Química Analítica, Universidad de Jaén, Campus Las Lagunillas, s/n, 23071, Jaén (Spain).

[c] Departamento de Química Orgánica e Inorgánica, Facultad de Ciencia y Tecnología, Universidad del País Vasco UPV/EHU, P.O. Box 644, 48080 Bilbao, Spain.

[d] National High Magnetic Field Laboratory, Florida State University, Tallahassee, Florida 32310, USA.

Table of Contents

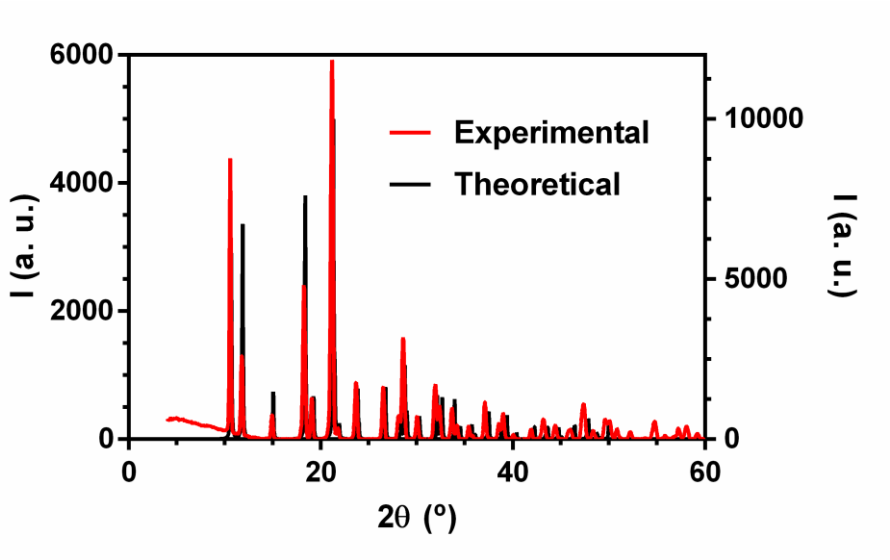

Figure S1. Theoretical (black line) and experimental (red line) X-Ray powder diffraction diagrams of compound **1**.

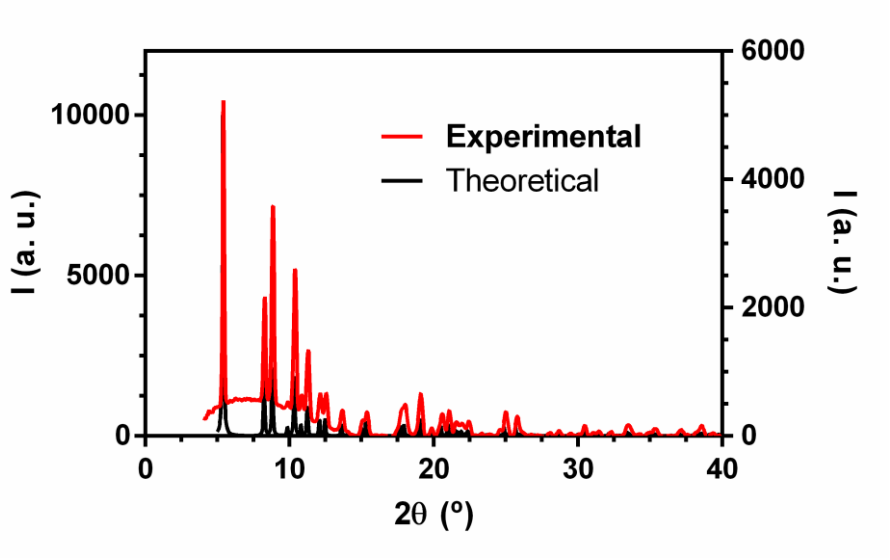

Figure S2. Theoretical (black line) and experimental (red line) X-Ray powder diffraction diagrams of compound **2**.

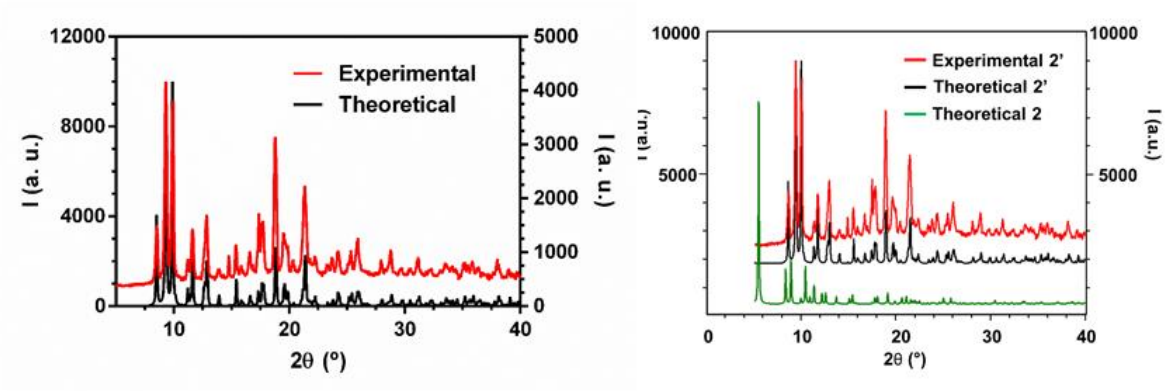

Figure S3. (Left) Theoretical (black line) and experimental (red line) X-Ray powder diffraction diagrams of compound **2'**. (Right) Comparison of these X-ray powder diffraction diagrams with the theoretical one for **2** (green line).

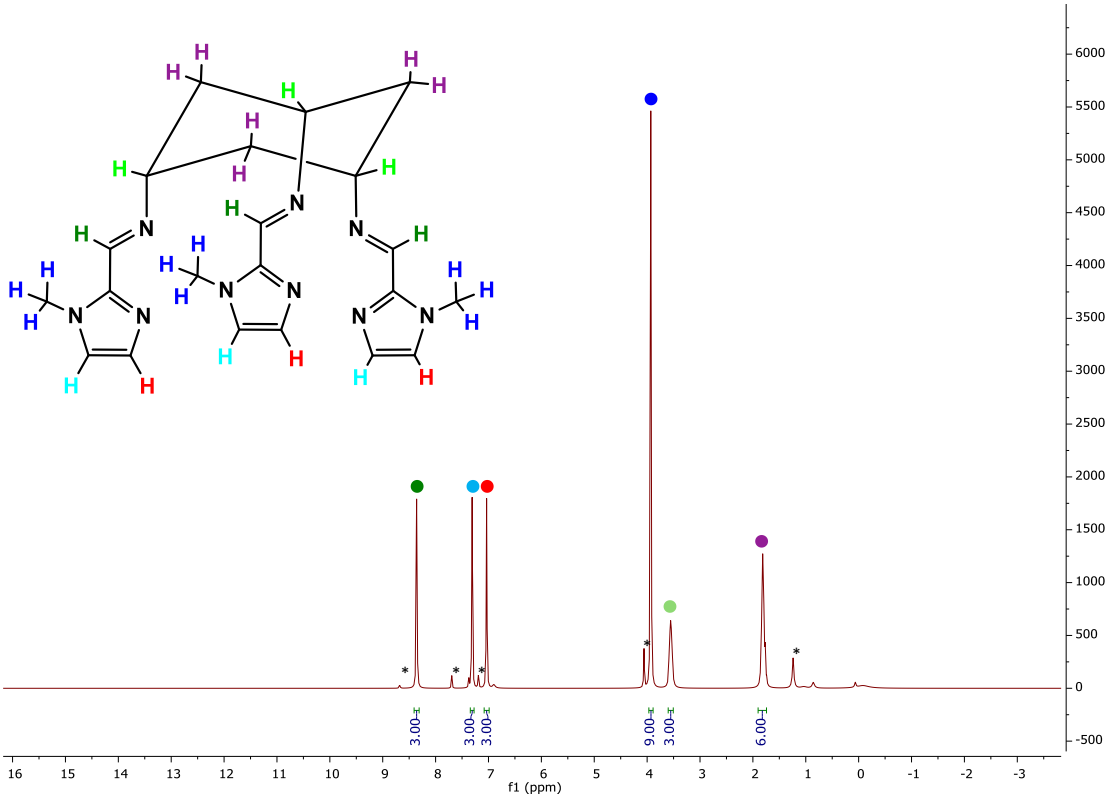

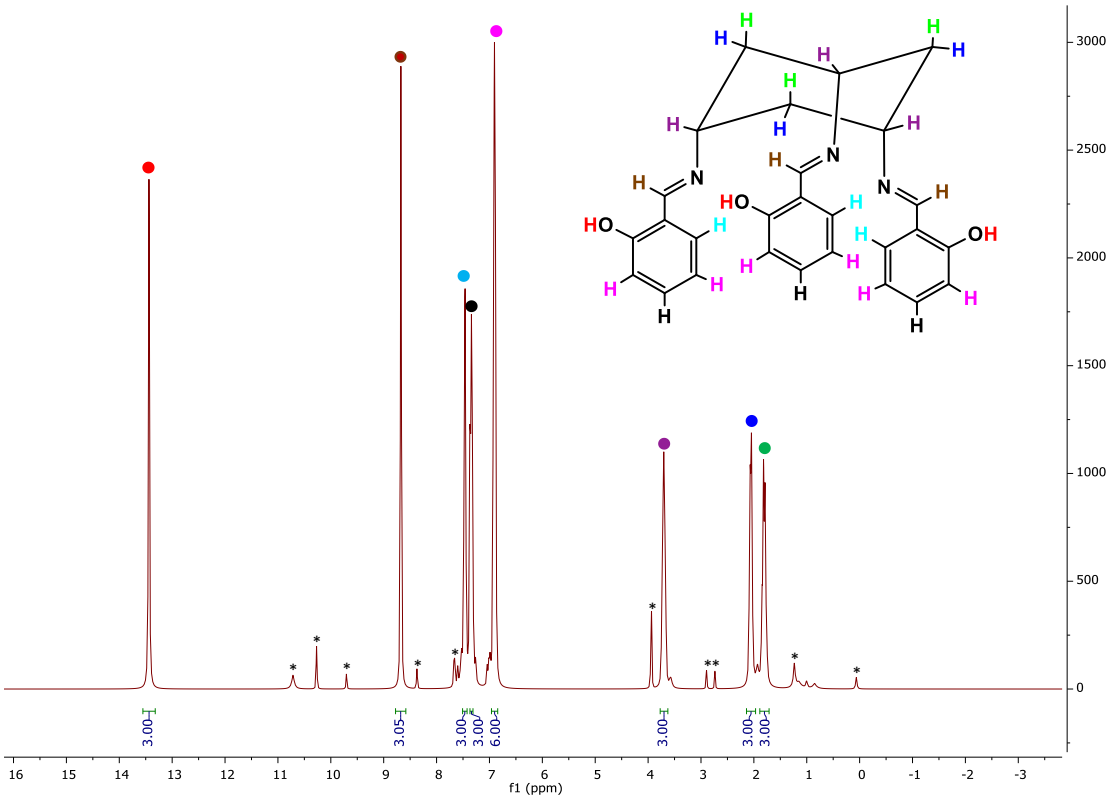

Figure S4.- (Top) ^{1}H NMR(400MHz, DMSO-d6,298K): 8.36 ppm (s,3H), 7.31 ppm (s,3H), 7.04 (s,3H), 3.93ppm (m,3H), 3.56 (m,3H),1.81 ppm(m,6H) of **L**.(Bottom) ^{1}H NMR(400MHz, DMSO-d6,298K): 13.44ppm (s,3H), 8.67 ppm (s,3H), 7.45 (m,3H), 7.35ppm (m,3H), 6.90ppm (m,6H), 3.70 ppm (m,3H), 2.06 ppm (m,3H), 1.81(m,3H) of **H_3L1**. Very weak signals are due to small impurities.

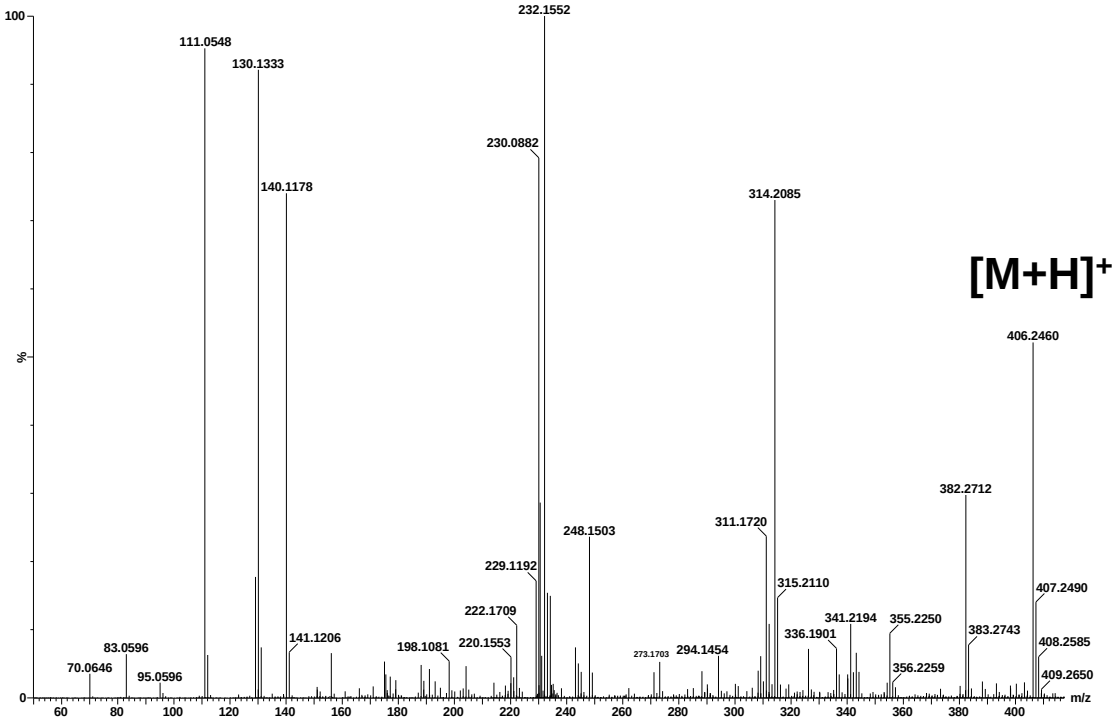

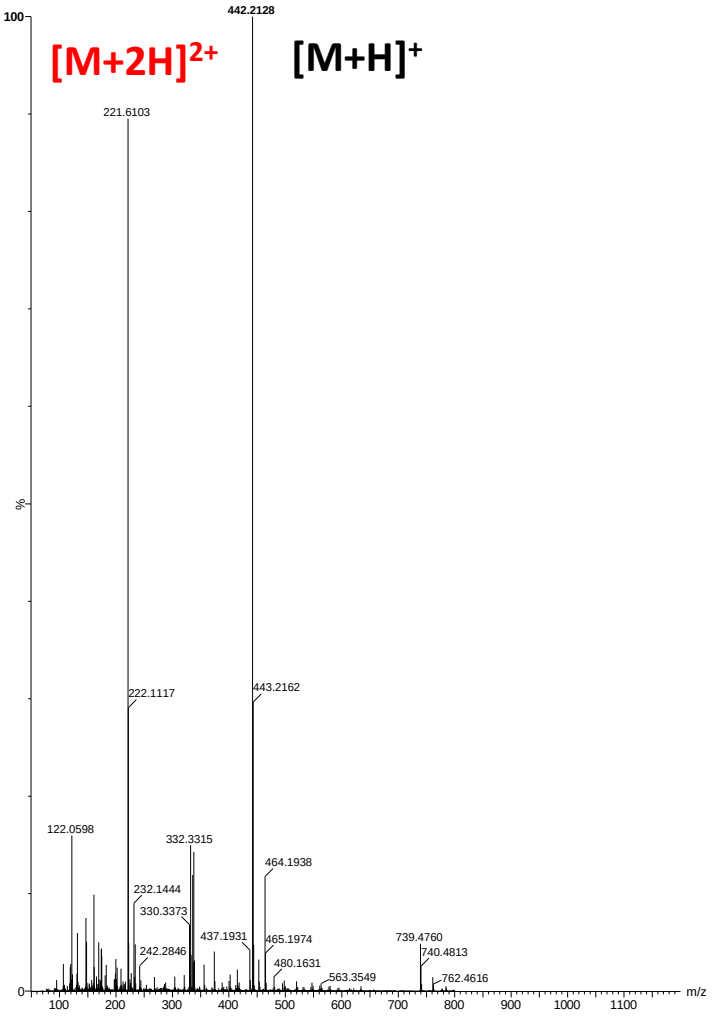

Figure S5. TOF-MS ES+ mass spectra of **L** (top) and **H_3L1** (botton). Very weak peaks at m/z larger than $[M+H]^+$ might be assigned to adduct/reactions in the ion source and/or impurities.

Table S1.- Crystal data and structure refinement for 1. CCDC2497812

Identification code	**1**
Empirical formula	$C_{42}H_{54}Cl_4Co_2N_{18}O_{16}$
Formula weight	7960.13
Temperature/K	120.00
Crystal system	trigonal
Space group	P31c
a/Å	9.650
b/Å	9.650
c/Å	16.570
α/°	90
β/°	90
γ/°	120
Volume/Å^3	1336.4
Z	1
ρ_{calc}g/cm^3	1.649
μ/mm^{-1}	0.907
F(000)	682
Crystal size/mm^3	0.158 × 0.075 × 0.059
Radiation	MoKα (λ = 0.71073)
2Θ range for data collection/°	4.874 to 56.590
Index ranges	$-12 \leq h \leq 12$, $-12 \leq k \leq 12$, $-18 \leq l \leq 22$
Reflections collected	13332
Independent reflections	2049 [R_{int} = 0.0383, R_{sigma} = 0.0348]
Data/restraints/parameters	2049/1/126
Goodness-of-fit on F^2	1.082
Final R indexes [I>=2σ (I)]	R_1 = 0.0248, wR_2 = 0.0563
Final R indexes [all data]	R_1 = 0.0279, wR_2 = 0.0587
Largest diff. peak/hole / e Å^{-3}	0.317/-0.236
Flack parameter	0.033(8)

Table S2.- Crystal data and structure refinement for 2'.
CCDC2497813

Identification code	**2'**
Empirical formula	$C_{54}H_{48}Co_3N_6O_6$
Formula weight	1053.77
Temperature/K	170.00(10)
Crystal system	triclinic
Space group	P-1
a/Å	11.1887(4)
b/Å	11.3205(2)
c/Å	18.2442(4)
α/°	101.190(2)
β/°	90.415(2)
γ/°	90.035(2)
Volume/Å^3	2266.85(10)
Z	2
ρ_{calc}g/cm^3	1.544
μ/mm^{-1}	1.146
F(000)	1086
Crystal size/mm^3	0.280 × 0.157 × 0.076
Radiation	MoKα (λ = 0.71073)
2Θ range for data collection/°	1.972 to 29.51
Index ranges	$-15 \leq h \leq 15$, $-15 \leq k \leq 12$, $-23 \leq l \leq 24$
Reflections collected	31177
Independent reflections	11016 [R_{int} = 0.0495, R_{sigma} = 0.0774]
Data/restraints/parameters	8214/0/625
Goodness-of-fit on F^2	1.102
Final R indexes [I>=2σ (I)]	R_1 = 0.0867, wR_2 = 0.2299
Final R indexes [all data]	R_1 = 0.1065, wR_2 = 0.2386
Largest diff. peak/hole / e Å^{-3}	2.034/-0.862

Table S3.- Crystal data and structure refinement for 2. CCDC2497814

Identification code	**2**
Empirical formula	$C_{60}H_{62}Co_3N_8O_8$
Formula weight	1199.96
Temperature/K	170.00(10)
Crystal system	cubic
Space group	Ia-3d
a/Å	40.1409(2)
b/Å	40.1409(2)
c/Å	40.1409(2)
α/°	90
β/°	90
γ/°	90
Volume/Å^3	64678.60(11)
Z	48
ρ_{calc}g/cm^3	1.479
μ/mm^{-1}	0.978
F(000)	29904
Crystal size/mm^3	0.216 × 0.109 × 0.061
Radiation	MoKα (λ = 0.71073)
2Θ range for data collection/°	2.259 to 25.965
Index ranges	-54 ≤ h ≤ 55, -51 ≤ k ≤ 54, -55 ≤ l ≤ 53
Reflections collected	362611
Independent reflections	7676 [R_{int} = 0.1192, R_{sigma} = 0.1585]
Data/restraints/parameters	3992/0/312
Goodness-of-fit on F^2	1.021
Final R indexes [I>=2σ (I)]	R_1 = 0.0590, wR_2 = 0.1461
Final R indexes [all data]	R_1 = 0.1225, wR_2 = 0.1756
Largest diff. peak/hole / e Å^{-3}	1.099/-0.278

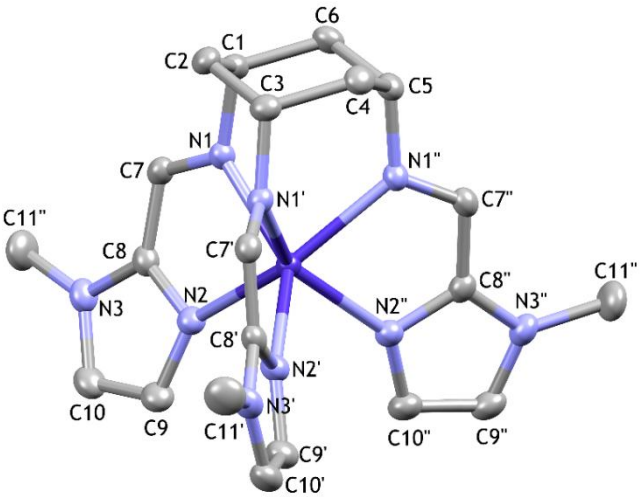

Scheme 1. Atom labelling used for **1** in the tables S4 and S5.

Table S4.- Bond Lengths for 1

Atom	Atom	Length/Å	Atom	Atom	Length/Å
Co1	N1[1]	2.162(2)	Cl1	O1CL[1]	1.431(2)
Co1	N1[2]	2.162(2)	N1	C2	1.471(3)
Co1	N1	2.162(2)	N1	C3	1.276(3)
Co1	N2[1]	2.165(2)	N2	C4	1.334(3)
Co1	N2[2]	2.165(2)	N2	C5	1.364(3)
Co1	N2	2.165(2)	N3	C4	1.352(3)
Cl2	O1	1.413(5)	N3	C6	1.371(4)
Cl2	O2[3]	1.423(3)	N3	C7	1.461(4)
Cl2	O2[4]	1.423(3)	C4	C3	1.446(4)
Cl2	O2	1.423(3)	C2	C1[2]	1.527(3)
Cl1	O2CL	1.441(4)	C2	C1	1.534(4)
Cl1	O1CL	1.431(2)	C5	C6	1.377(4)
Cl1	O1CL[2]	1.431(2)			

Symmetry codes: [1]1+Y-X,1-X,+Z; [2]1-Y,+X-Y,+Z; [3]2-Y,1+X-Y,+Z; [4]1+Y-X,2-X,+Z

Table S5.- Bond Angles for 1

Atom	Atom	Atom	Angle/°	Atom	Atom	Atom	Angle/°
N1[1]	Co1	N1[2]	81.98(8)	O1CL[2]	Cl1	O2CL	109.17(12)
N1[1]	Co1	N1	81.98(8)	O1CL	Cl1	O1CL[2]	109.77(12)
N1[2]	Co1	N1	81.98(8)	O1CL[1]	Cl1	O1CL	109.77(12)
N1[1]	Co1	N2[1]	76.18(8)	O1CL[1]	Cl1	O1CL[2]	109.77(12)
N1[2]	Co1	N2[1]	123.71(7)	C2	N1	Co1	124.49(16)
N1	Co1	N2[1]	142.52(8)	C3	N1	Co1	116.59(17)
N1[1]	Co1	N2[2]	142.52(8)	C3	N1	C2	118.4(2)
N1[2]	Co1	N2[2]	76.18(8)	C4	N2	Co1	111.34(17)
N1	Co1	N2[2]	123.71(7)	C4	N2	C5	106.3(2)
N1[1]	Co1	N2	123.71(8)	C5	N2	Co1	142.32(18)
N1[2]	Co1	N2	142.52(8)	C4	N3	C6	106.8(2)
N1	Co1	N2	76.18(8)	C4	N3	C7	126.9(3)
N2[1]	Co1	N2	91.07(8)	C6	N3	C7	126.3(2)
N2[1]	Co1	N2[2]	91.07(8)	N2	C4	N3	111.2(2)
N2[2]	Co1	N2	91.07(8)	N2	C4	C3	120.6(2)
O1	Cl2	O2[3]	109.55(14)	N3	C4	C3	128.0(2)
O1	Cl2	O2[4]	109.55(14)	N1	C2	C1	108.6(2)
O1	Cl2	O2	109.55(14)	N1	C2	C1[2]	111.0(2)
O2[3]	Cl2	O2	109.39(14)	C1[2]	C2	C1	110.8(2)
O2[4]	Cl2	O2	109.39(14)	N2	C5	C6	109.0(2)
O2[3]	Cl2	O2[4]	109.39(14)	C2[1]	C1	C2	113.4(2)
O1CL[1]	Cl1	O2CL	109.17(12)	N1	C3	C4	115.2(2)
O1CL	Cl1	O2CL	109.17(12)	N3	C6	C5	106.7(2)

Symmetry codes: [1]1+Y-X,1-X,+Z; [2]1-Y,+X-Y,+Z; [3]2-Y,1+X-Y,+Z; [4]1+Y-X,2-X,+Z

Table S6.- SHAPE Calculations for compound **1**.

```
-------------------------------------------------------------------------
S H A P E   v2.1         Continuous Shape Measures calculation
(c) 2013  Electronic Structure Group, Universitat de Barcelona
                   Contact:  llunell@ub.edu
-------------------------------------------------------------------------

JPPY-6           5 C5v   Johnson pentagonal pyramid J2
TPR-6            4 D3h   Trigonal prism
OC-6             3 Oh    Octahedron
PPY-6            2 C5v   Pentagonal pyramid
HP-6             1 D6h   Hexagon

Structure [ML6 ]    JPPY-6      TPR-6       OC-6      PPY-6       HP-6
 Co1                21.415,    1.198,      10.814,   17.232,    35.957
```

Table S7. Co–O and Co–N distances (Å) in **2'**.

Co1A	d (Å)	**Co2A**	d (Å)	**Co1A^{ii}**	d (Å)
Co1A–O18A	2.120(5)	Co2A–O18A	2.125(4)	Co1A^{ii}–O18A^{ii}	2.120(5)
Co1A–O38A	2.115(5)	Co2A–O38A	2.081(4)	Co1A^{ii}–O38A^{ii}	2.115(5)
Co1A–O58A	2.121(4)	Co2A–O58A	2.075(4)	Co1A^{ii}–O58A^{ii}	2.121(4)
Co1A–N1A	2.143(6)	Co2A–O18A^{ii}	2.125(4)	Co1A^{ii}–N1A^{ii}	2.143(6)
Co1A–N3A	2.148(6)	Co2A–O38A^{ii}	2.081(4)	Co1A^{ii}–N3A^{ii}	2.148(6)
Co1A–N5A	2.136(5)	Co2A–O58A^{ii}	2.075(4)	Co1A^{ii}–N5A^{ii}	2.136(5)
Co1B	d (Å)	**Co2B**	d (Å)	**Co1B^{iii}**	d (Å)
Co1B–O18B	2.118(5)	Co2B–O18B	2.082(4)	Co1Bii^{i}–O18B^{iii}	2.118(5)
Co1B–O38B	2.113(4)	Co2B–O38B	2.082(4)	Co1Bii^{i}–O38B^{iii}	2.113(4)
Co1B–O58B	2.106(5)	Co2B–O58B	2.094(5)	Co1B^{iii}–O58B^{iii}	2.106(5)
Co1B–N1B	2.136(5)	Co2B–O18B^{iii}	2.082(4)	Co1B^{iii}–N1B^{iii}	2.136(5)
Co1B–N3B	2.141(6)	Co2B–O38B^{iii}	2.082(4)	Co1B^{iii}–N3B^{iii}	2.141(6)
Co1B–N5B	2.153(5)	Co2B–O58B^{iii}	2.094(5)	Co1B^{iii}–N5B^{iii}	2.153(5)

Symmetry codes: ii) 2–x, –y, 1–z; iii) 1–x, 1–y, 2–z.

Table S8.- Bond Angles for **2'**.

Atom	Atom	Atom	Angle/°	Atom	Atom	Atom	Angle/°
N1A	Co1A	O18A	84.0(2)	N1B	Co1B	O18B	84.27(19)
N1A	Co1A	O38A	124.9(2)	N1B	Co1B	O38B	147.2(2)
N1A	Co1A	O58A	146.1(2)	N1B	Co1B	O58B	122.6(2)
N1A	Co1A	N3A	87.5(2)	N1B	Co1B	N3B	87.9(2)
N1A	Co1A	N5A	88.6(2)	N1B	Co1B	N5B	88.3(2)
N3A	Co1A	O18A	146.2(2)	N3B	Co1B	O18B	124.7(2)
N3A	Co1A	O38A	83.3(2)	N3B	Co1B	O38B	84.08(19)
N3A	Co1A	O58A	124.4(2)	N3B	Co1B	O58B	147.5(2)
N3A	Co1A	N5A	85.9(2)	N3B	Co1B	N5B	86.4(2)
N5A	Co1A	O18A	126.4(2)	N5B	Co1B	O18B	147.5(2)
N5A	Co1A	O38A	144.0(2)	N5B	Co1B	O38B	122.7(2)
N5A	Co1A	O58A	83.13(19)	N5B	Co1B	O58B	83.8(2)
O18A	Co1A	O38A	75.17(18)	O18B	Co1B	O38B	74.64(19)
O18A	Co1A	O58A	74.89(18)	O18B	Co1B	O58B	73.92(19)
O38A	Co1A	O58A	75.15(18)	O38B	Co1B	O58B	75.5(2)
O18A	Co2A	O38A	75.78(19)	O18B	Co2B	O38B	76.04(19)
O18A	Co2A	O58A	75.75(18)	O18B	Co2B	O58B	74.9(2)
O18A	Co2A	O18A^{ii}	180.0	O18B	Co2B	O18B^{iii}	180.0
O18A	Co2A	O38A^{ii}	104.21(19)	O18B	Co2B	O38B^{iii}	103.96(19)
O18A	Co2A	O58A^{ii}	104.25(18)	O18B	Co2B	O58B^{iii}	105.1(2)
O38A	Co2A	O58A	76.86(18)	O38B	Co2B	O58B	76.43(19)
O38A	Co2A	O18A^{ii}	104.21(19)	O38B	Co2B	O18B^{iii}	103.96(19)
O38A	Co2A	O38A^{ii}	180.0	O38B	Co2B	O38B^{iii}	180.0
O38A	Co2A	O58A^{ii}	103.14(18)	O38B	Co2B	O58B^{iii}	103.56(19)
O58A	Co2A	O18A^{ii}	104.25(18)	O58B	Co2B	O18B^{iii}	105.1(2)
O58A	Co2A	O38A^{ii}	103.14(18)	O58B	Co2B	O38B^{iii}	103.56(19)
O58A	Co2A	O58A^{ii}	180.0(4)	O58B	Co2B	O58B^{iii}	180.0
N1A^{ii}	Co1A^{ii}	O18A^{ii}	84.0(2)	N1B^{iii}	Co1B^{iii}	O18B^{iii}	84.27(19)
N1A^{ii}	Co1A^{ii}	O38A^{ii}	124.9(2)	N1B^{iii}	Co1B^{iii}	O38B^{iii}	147.2(2)
N1A^{ii}	Co1A^{ii}	O58A^{ii}	146.1(2)	N1B^{iii}	Co1B^{iii}	O58B^{iii}	122.6(2)
N1A^{ii}	Co1A^{ii}	N3A^{ii}	87.5(2)	N1B^{iii}	Co1B^{iii}	N3B^{iii}	87.9(2)
N1A^{ii}	Co1A^{ii}	N5A^{ii}	88.6(2)	N1B^{iii}	Co1B^{iii}	N5B^{iii}	88.3(2)
N3A^{ii}	Co1A^{ii}	O18A^{ii}	146.2(2)	N3B^{iii}	Co1B^{iii}	O18B^{iii}	124.7(2)
N3A^{ii}	Co1A^{ii}	O38A^{ii}	83.3(2)	N3B^{iii}	Co1B^{iii}	O38B^{iii}	84.08(19)
N3A^{ii}	Co1A^{ii}	O58A^{ii}	124.4(2)	N3B^{iii}	Co1B^{iii}	O58B^{iii}	147.5(2)
N3A^{ii}	Co1A^{ii}	N5A^{ii}	85.9(2)	N3B^{iii}	Co1B^{iii}	N5B^{iii}	86.4(2)
N5A^{ii}	Co1A^{ii}	O18A^{ii}	126.4(2)	N5B^{iii}	Co1B^{iii}	O18B^{iii}	147.5(2)
N5A^{ii}	Co1A^{ii}	O38A^{ii}	144.0(2)	N5B^{iii}	Co1B^{iii}	O38B^{iii}	122.7(2)
N5A^{ii}	Co1A^{ii}	O58A^{ii}	83.13(19)	N5B^{iii}	Co1B^{iii}	O58B^{iii}	83.8(2)
O18A^{ii}	Co1A^{ii}	O38A^{ii}	75.17(18)	O18B^{iii}	Co1B^{iii}	O38B^{iii}	74.64(19)
O18A^{ii}	Co1A^{ii}	O58A^{ii}	74.89(18)	O18B^{iii}	Co1B^{iii}	O58B^{iii}	73.92(19)
O38A^{ii}	Co1A^{ii}	O58A^{ii}	75.15(18)	O38B^{iii}	Co1B^{iii}	O58B^{iii}	75.5(2)
Co1A	O18A	Co2A	89.03(17)	Co1B	O18B	Co2B	90.32(17)
Co1A	O38A	Co2A	90.32(18)	Co1B	O38B	Co2B	90.44(17)
Co1A	O58A	Co2A	90.32(17)	Co1B	O58B	Co2B	90.31(19)
Co1A	Co2A	Co1A^{ii}	180.0	Co1B	Co2B	Co1B^{iii}	180.0

Symmetry codes: ii) 2–x, –y, 1–z; iii) 1–x, 1–y, 2–z.

Table S9. Co···Co distances (Å) in **2** and **2'**.

Co···Co in **2**			Co···Co in **2'**		
Co1···Co2	2.9744(3)	Co1A···Co2A	2.9759(8)	Co1B···Co2B	2.9782(8)
Co2···Co1[i]	2.9744(3)	Co2A···Co1A[ii]	2.9759(8)	Co2B···Co1B[iii]	2.9782(8)

Symmetry codes: i) 5/4 – y, 5/4 – x, ¼ – z; ii) 2–x, –y, 1–z; iii) 1–x, 1–y, 2–z.

Table S10.- SHAPE Calculations for compound **2'**.

Molecule A

```
-----------------------------------------------------------------
S H A P E   v2.1         Continuous Shape Measures calculation
(c) 2013  Electronic Structure Group, Universitat de Barcelona
                  Contact:  llunell@ub.edu
-----------------------------------------------------------------

JPPY-6          5 C5v   Johnson pentagonal pyramid J2
TPR-6           4 D3h   Trigonal prism
OC-6            3 Oh    Octahedron
PPY-6           2 C5v   Pentagonal pyramid
HP-6            1 D6h   Hexagon

Structure [ML6 ]    JPPY-6      TPR-6       OC-6       PPY-6       HP-6
 Co1               21.345,     1.235,     10.495,    17.574,    33.865
 Co1'              21.355,     1.237,     10.493,    17.567,    33.876
 Co2               32.059,     14.304,    2.643,     29.240,    29.035
```

Molecule B

```
Structure [ML6 ]    JPPY-6      TPR-6       OC-6       PPY-6       HP-6
 Co1               21.914,     1.669,      9.449,     17.622,    34.330
 Co1'              21.912,     1.669,      9.449,     17.625,    34.321
 Co2               31.736,     14.290,     2.768,     29.048,    29.026
```

Crystal Structure of compound 2.

Compound **2** crystallizes in the cubic Ia-3d space group, and its asymmetric unit contains one half of the $[(CoL1)_2Co]$ cobalt(II)-complex and 2 DMF solvent molecules. Although DMF solvent molecules could not be modelled from the Fourier map, the solvent accessible void volume in compound 2 is consistent with the presence of two DMF molecules per unit cell. Therefore, the diffraction intensities of the disordered solvent were treated using the SQUEEZE routine as implemented in PLATON and the presence of two DMF solvent molecules were included in the final formula. The structure of compound **2** can be described as a linear centrosymmetric tricobalt complex, which exhibits a virtually identical arrangement as in 2' (see Figure 2). The peripheral Co(II) centers, named Co(1), exhibit a CoN_3O_3 coordination sphere composed by the imine nitrogen and the phenoxide oxygen atoms, whereas the central Co(II) ion, named Co(2), is coordinated to both $L1^{3-}$ ligands through the phenoxide oxygen groups, leading to a CoO_6 coordination sphere. Mean Co–N and Co–O bond distances (Table S11) and angles (Table S12) are consistent with the ones found in 2' and other Co(II) complexes with this kind of donor atoms; Co(1)–N, 2.122-2.144 Å; Co(1)–O 2.105-2.130 Å and Co(2)–O 2.062 Å-2.098 Å ranges. Continuous shape measurements (Table S13) indicate that the coordination sphere of the cobalt(II) centres coincide with those found in 2', exhibiting the peripheral Co(1) ions a symmetry close to an ideal TPR-6 polyhedron (TPR-6 = 1.221, OC-6 10.720, % path deviation of 5.2) and the central Co(2) being close to an ideal octahedral

geometry (SOC-6 = 3.019, TPR-6 = 10.75). The organic ligands on compound 2 exhibits the same arrangement as in 2', in which the arms of the two coordinated ligands are found rotated by 60° one from each other (Figure 2), which can be viewed from the pseudo-C_3 axis running along the Co-Co-Co trinuclear center. Finally, the mean shortest intramolecular Co(1)···Co(2) and Co(1)···Co(1) distances are found to be 2.974 and 5.947 Å, respectively (Table S9).

In summary, the main differences between 2' and the related complex [{Co(μ-L')}$_2$Co] (2) (where L' = 1,1,1-tris[(salicylideneamino)methyl]ethane) are: (i) The CoN_3O_6 coordination environment of the external Co(II) ions is closer to an ideal TPR- geometry in the former than in the latter, (ii) The Co(2) central ion, however, is slightly more distorted from the ideal OC-6 geometry in compound 2, (iii) the Co(1)···Co(1) and Co(1)···Co(2) distances are both slightly larger in 2 and, consequently, the Co(1)-O-Co(1) bridging angles (mean value of 90.1° for the former and 88.3° for the latter), (iv) the θ angle between the N3 and O3 triangular parallel faces is larger for the former (12.42°) than for the latter (9.7°), whereas the mean ϕ angles between the Co(1)-O-Co(2) plane and the plane of the phenyl ring is larger for the latter than for the former.

Table S11. Co–O and Co–N distances (Å) in **2**.

Co1	d (Å)	**Co2**	d (Å)	**Co1^i**	d (Å)
Co1–O18	2.105(2)	Co2–O18	2.062(2)	Co1^i–O18^i	2.105(2)
Co1–O38	2.130(3)	Co2–O38	2.088(3)	Co1^i–O38^i	2.130(3)
Co1–O58	2.113(2)	Co2–O58	2.098(2)	Co1^i–O58^i	2.113(2)
Co1–N1	2.144(3)	Co2–O18^i	2.062(2)	Co1^i–N1^i	2.144(3)
Co1–N3	2.122(3)	Co2–O38^i	2.088(3)	Co1^i–N3^i	2.122(3)
Co1–N5	2.130(3)	Co2–O58^i	2.098(2)	Co1^i–N5^i	2.130(3)

Symmetry codes: i) 5/4 – y, 5/4 – x, ¼ – z.

Table S12.- Bond Angles for 2

Atom	**Atom**	**Atom**	**Angle/°**	**Atom**	**Atom**	**Atom**	**Angle/°**
N1	Co1	O18	83.45(11)	O38	Co2	O58^i	173.65(11)
N1	Co1	O38	125.11(13)	O58	Co2	O18^i	99.34(10)
N1	Co1	O58	146.56(11)	O58	Co2	O38^i	173.65(11)
N1	Co1	N3	86.39(13)	O58	Co2	O58^i	108.28(13)
N1	Co1	N5	88.03(13)	N1^i	Co1^i	O18^i	83.45(11)
N3	Co1	O18	143.27(13)	N1^i	Co1^i	O38^i	125.11(13)
N3	Co1	O38	83.30(12)	N1^i	Co1^i	O58^i	146.56(11)
N3	Co1	O58	125.52(12)	N1^i	Co1^i	N3^i	86.39(13)
N3	Co1	N5	89.10(14)	N1^i	Co1^i	N5^i	88.03(13)
N5	Co1	O18	125.56(12)	N3^i	Co1^i	O18^i	143.27(13)
N5	Co1	O38	145.16(12)	N3^i	Co1^i	O38^i	83.30(12)
N5	Co1	O58	83.30(11)	N3^i	Co1^i	O58^i	125.52(12)
O18	Co1	O38	74.19(11)	N3^i	Co1^i	N5^i	89.10(14)
O18	Co1	O58	75.76(9)	N5^i	Co1^i	O18^i	125.56(12)
O38	Co1	O58	73.97(10)	N5^i	Co1^i	O38^i	145.16(12)
O18	Co2	O38	76.00(10)	N5^i	Co1^i	O58^i	83.30(11)
O18	Co2	O58	77.00(9)	O18^i	Co1^i	O38^i	74.19(11)
O18	Co2	O18^i	173.87(16)	O18^i	Co1^i	O58^i	75.76(9)
O18	Co2	O38^i	108.01(10)	O38^i	Co1^i	O58^i	73.97(10)
O18	Co2	O58^i	99.34(10)	Co1	O18	Co2	91.08(9)
O38	Co2	O58	75.13(11)	Co1	O38	Co2	89.69(10)
O38	Co2	O18^i	108.02(10)	Co1	O58	Co2	89.87(9)

Table S12.- Bond Angles for 2

Atom	Atom	Atom	Angle/°	Atom	Atom	Atom	Angle/°
O38	Co2	O38^{i}	102.00(17)	Co1	Co2	Co1^{i}	178.01(3)

Symmetry codes: i) 5/4 – y, 5/4 – x, ¼ – z.

Table S13.- SHAPE Calculations for compound **2**.

```
-----------------------------------------------------------------
S H A P E    v2.1           Continuous Shape Measures calculation (c)
2013     Electronic   Structure   Group,   Universitat   de   Barcelona
Contact:  llunell@ub.edu
-----------------------------------------------------------------
HP-6        1 D6h       Hexagon
PPY-6       2 C5v       Pentagonal pyramid
OC-6        3 Oh        Octahedron
TPR-6       4 D3h       Trigonal prism
JPPY-6      5 C5v       Johnson pentagonal pyramid J2

Structure [ML6 ]     HP-6       PPY-6       OC-6       TPR-6      JPPY-6
 Co1                      33.820,      17.262,      10.675,      1.221,
21.208
 Co1                      33.820,      17.262,      10.675,      1.221,
21.208
 Co2                     29.402,      26.547,      3.019,       10.720,
29.893
```

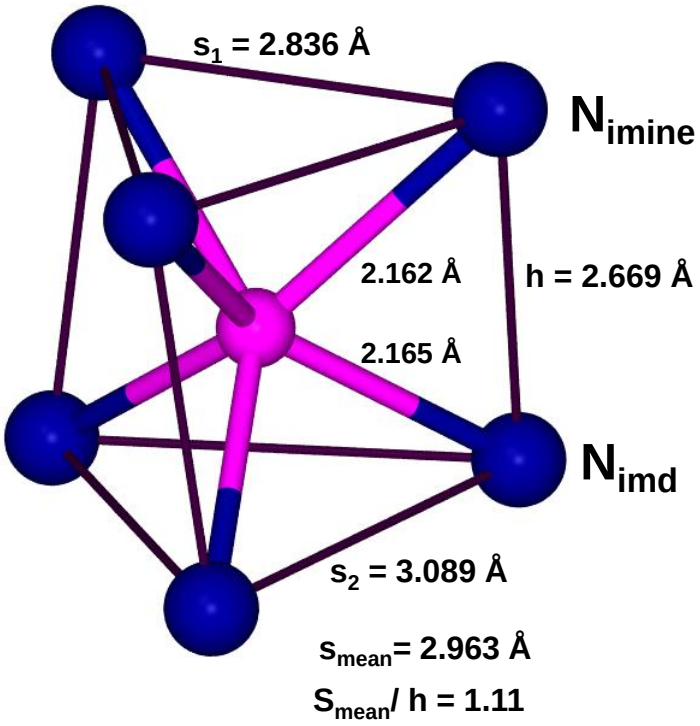

Figure S6. CoN_6 coordination sphere of **1** including some structural parameters.

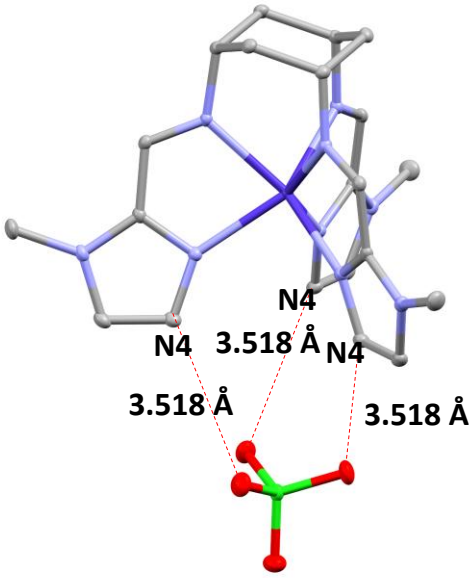

Figure S7. Interactions between the perchlorate anion and the hydrogen atoms bonded to the N4 imidazole atoms.

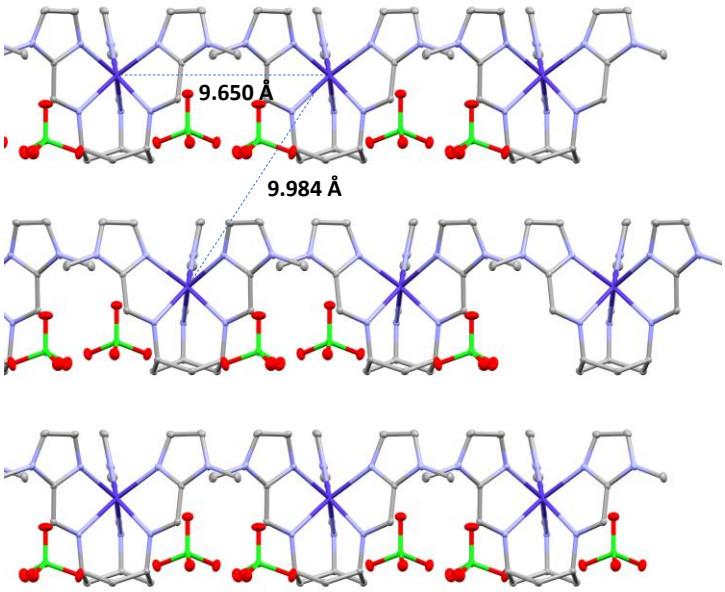

Figure S8.- Packing of compound **1** including the shortest intermolecular Co···Co distances.

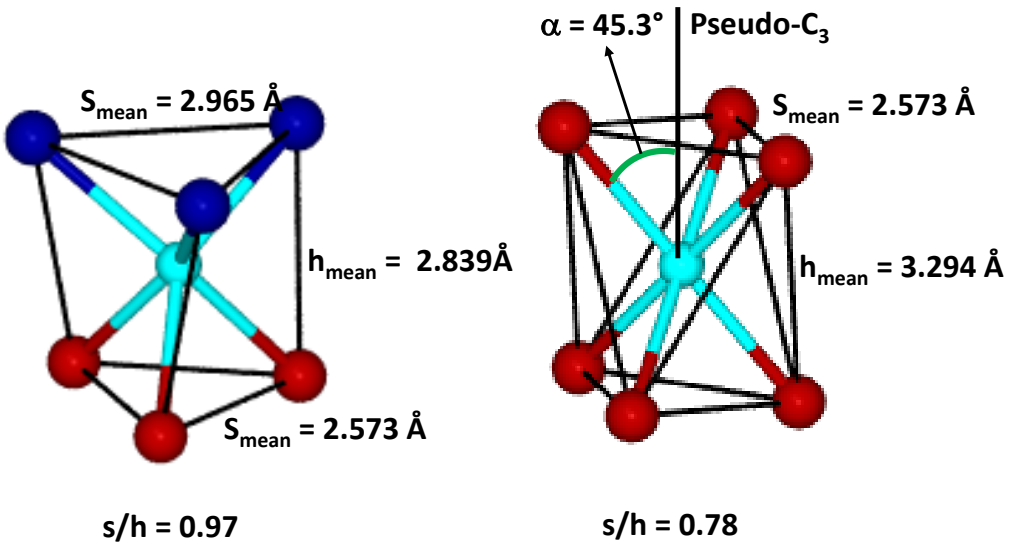

Figure S9.- CoN_3O_3 and CoO_6 coordination spheres for **2**, including some structural parameters.

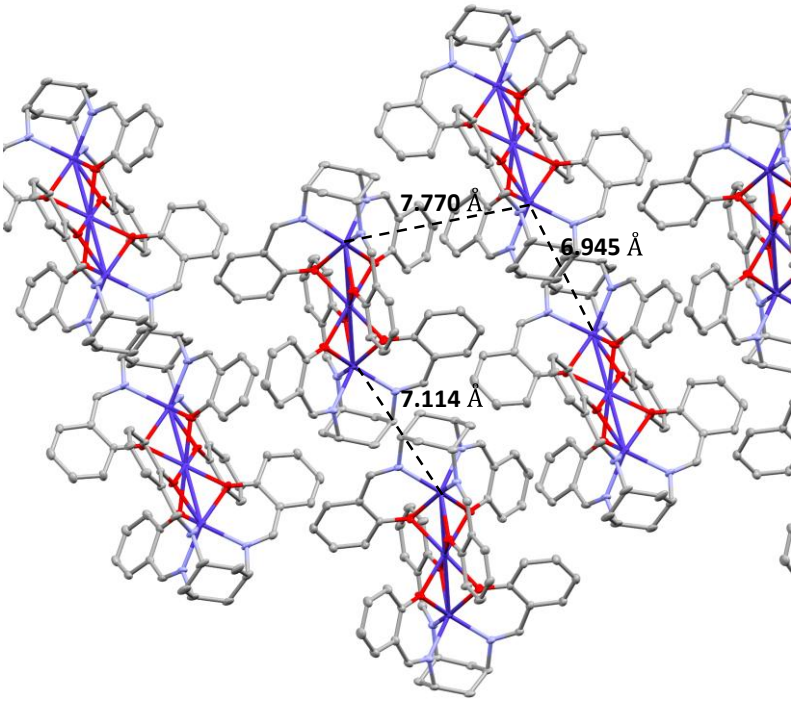

Figure S10.- Packing of compound **2** including the shortest intermolecular Co···Co distances.

Table S14.- Experimental anisotropy parameters (extracted from ZFS and/or GF Hamiltonians and FIRMS), continuous shape measures, slow magnetic relaxation (SMR) at zero field and hysteresis for selected hexacoordinated Co(II) MSMMs with local geometry closer to trigonal prismatic.

Compound	D_{exp}/cm^{-1}	$\|E_{exp}\|$	Δ_{ax}/cm^{-1}	$\|\Delta_{rh}\|$/cm^{-1}	SOC6/STPR6	SMR (H_{dc} = 0)/ U_{eff} (cm^{-1})	Hysteresis (2 K)	Ref
[Co (PStMeImid)][BF_4]$_2$*	-98.9 (-114)[a]	b			13.9/0.49	Yes/26	Yes[c]	1
[Co (PStMeImid)][ClO_4]$_2$*	-95.2 (-114)[a]	b			13.6/0.53	Yes/28	Yes[c]	1
[Co (tppm*)][BPh_4]$_2$	-97.2	0.009			15.9/0.55	Yes/123	Yes[d]	2
[Co(tppm)][ClO_4]$_2$·2CH_3CN·H_2O	-80.7	0.6			14.9/0.59	Yes/39	Yes[d]	3
[Co($TzOx$)$_3$(BC_6H_5)Cl]			-602.4	94.3	16.8/0.73	Yes/44	N.R.	4
[Co($PzOx$)$_3$(BC_6H_5)]Cl	-82.0	0.25			16.3/0.83	Yes/49	Yes	5
[Co($PzOx$)$_3$($BC_{16}H33$)]Cl(α-Co)	-111	b			15.8/0.81	Yes/180	Yes	6
[Co($PzOx$)$_3$($BC_{16}H33$)]Cl(β-Co)	-74.1	b			16.3/0.87	Yes/109	Yes	6
[Co($AcPzOx$)$_3$(BC_6H_5)DMF]$_2$ ($B_{10}Cl_{10}$)	-85.2	b			15.2/0.86	Yes/128	N.R.	7
[Co($PSImid$)$_3$](NO_3)$_2$	-72	7			11.9/0.87	Yes/23	N.R.	8
[Co($AcMeImd$)$_3$BPh]ClO_4	-102.5[a]	b			13.5/0.90	Yes/51	Yes	9
[Co(tamcyMeImd)][BF_4]$_2$*	-108.1 (-108.5)[a]	0.08			10.18/1.20	Yes/27	Yes[d]	T.w.
[Co(pprz)]	-31	<0.001			10.9/1.38	Yes[e]/57 (H = 0.12 T)	N. R.	10
{Na[Co(tamcypy)]}(BPh_4)$_3$	-75.8	0.0001			9.3/1.79	Yes/50 (H = 0.1T)	No	11
[$CoTp^{py}$]PF_6			-1054.4	2.25	15.3/1.86	Yes/36	Yes	12
[Co($AcPyOx$)$_3$$BC_6H_5$]$ClO_4$	-86	b			10.0/2.00	Yes/45	N.R.	13
[$HNEt_3$][$Co^{II}Co^{III}_3$($bhpmp$)$_6$]	-115.9	2.8			9.5/2.22	Yes/76	No	14
[Co(hpy)][BPh_4]$_2$·3CH_2Cl_2	107.5	3.5			8.2/2.47	Yes/80	No	2
[Co ($PStpy$)][BF_4]$_2$	-127.6 (-100.5)[a]	0.22			7.4/2.76	Yes[e]/39	Yes[c]	15
[Co($PStpy$)][ClO_4]$_2$·CH_3OH	-116 (-97.5)[a]	3.1			7.3/3.02	Yes[e]/39	Yes[c]	15
[Co ($PStpy$)]$ZnCl_4$·CH_3OH	87.2 (-93.9)[a]	0.02			6.8/3.83	Yes[e]/35	Yes[c]	15
[Co($PStiso$)](ClO_4)$_2$·2CH_3OH	-80.9 (-105)[a]	0.02	-1668.9	1.77	5.6/4.32	Yes[e]/30 (H =0.15 T)	N.R.	16
[Co**L$_{diProp}$**(CH_3CN)](ClO_4)$_2$	-25.8	7.7			12.8/5.14	No/13 (H = 0.1 T)	N.R.	17
[Co($hdpym$)Cl_2]·H_2O			-1252.2	183.6	11.29/6.15	No/NR	N.R.	18
[Co(neo)(CH_3COO)$_2$]			-3317.1	133.0	11.8/3.76	No/26 (H = 0.1 T)	N.R.	19
[Co(fpa-en)]·MeOH	-30.3	5.2			16.8/1.63	No/51 (H = 0.1 T)	N.R.	20
[Co(fpa-pda)]·DMSO	-13.2	3.7			13.7/1.88	No/23 (H = 0.15 T)	N.R.	20
[Co(fpa-cn)]·MeOH	-30.5	6.3			17.8/1.91 12.7/1.47	No/35 (H = 0.15 T)	N.R.	20
[Co (abs)$_2$]·2H_2O	-47.4	0.001[f]			7.1/2.80	No/43 (H = 0.1T)	N. R.	21
[Co ($pabs$)$_2$]	-38.3	0.003f			8.2/2.34	No/39 (H = 0.1T)	N.R.	21

*These compounds have C_3 symmetry. [a] These values were determined by FIRMS. [b] In these cases *E* was fixed to zero. [c] The hysteresis was observed in pulse magnetization at 0.4 K. [d] Open hysteresis at zero dc field. T.w. represents this work. [e] Broad frequency dependent signal at very low temperature due to the

presence of significant QTM. N.R = Not reported. [f] The computed values of E/D are close to 0.1, which could justify the absence of SMR.

References of table S14

1.- A. Landart-Gereka, M. M. Quesada-Moreno, M. A. Palacios, I. F. Díaz-Ortega, H. Nojiri, M. Ozerov, J. Krzystek and E. Colacio, Pushing up the easy-axis magnetic anisotropy and relaxation times in trigonal prismatic Co^{II} mononuclear SMMs by molecular structure design, *Chem. Commun.*, 2023, **59**, 952–955.

2.- B. Yao, M. K. Singh, Y.-F. Deng, Y.-N. Wang, . R. Dunbar, Y.Z. Zhang, Trigonal Prismatic Co(II) Single-Ion Magnets: Manipulating the Magnetic Relaxation Through Symmetry Control, *Inorg. Chem*. 2020, **59**, 8505-8513.

3.- B. Yao, Y. F. Deng, T. Li, J. Xiong, B. W. Wang, Z. Zheng and Y. Y. Zhang, Construction and magnetic study of a trigonal-prismatic cobalt(II) single-ion magnet, *Inorg. Chem.,* 2018, **57**, 14047-14051.

4.- S. A. Belova, A. A. Danshina, A. S. Belov, A. S Bogomyakov, E. G Lebed, A. I. Dmitriev, P. V. Dorovatovskii, Y. Z. Voloshin, D. V Korchagin, Mikhail V Zhidkov, Synthesis, structure and magnetic properties of the monocapped 3d-metal(II) tris-N,S-heterocyclooximates: the design of cobalt pseudoclathrochelate with a single-ion magnet behavior, *Polyhedron*, 2026, **284**, 117860.

5.- V. V. Novikov, A. A. Pavlov, Y. V. Nelyubina, M. E. Boulon, O. A. Varzatskii, Y. Z. Voloshin, and R. E. P. Winpenny, A trigonal prismatic mononuclear cobalt(II) complex showing single-molecule magnet behaviour, *J. Am. Chem. Soc.,* 2015, **137**, 9792-9795.

6.- A. A. Pavlov, Y. V. Nelyubina , S. V. Kats , L. V. Penkova , N. N. Efimov , A. O. Dmitrienko , A. V. Vologzhanina , A. S. Belov , Y. Z. Voloshin and V. V. Novikov , Polymorphism in a Cobalt-Based Single-Ion Magnet Tuning Its Barrier to Magnetization Relaxation, *J. Phys. Chem. Lett.*, 2016, **7** , 4111 —4116.

7.- A. S. Belov, Y. Z. Voloshin, A. A. Pavlov, Y. V. Nelyubina, S. A. Belova, Y. V. Zubavichus, V. V. Avdeeva, N. N. Efimov, E. A. Malinina, K. Yu. Zhizhin, N. T. Kuznetsov, Solvent-Induced Encapsulation of Cobalt(II) Ion by a Boron-Capped tris-Pyrazoloximate, *Inorg. Chem*. 2020, **59**, 5845–5853.

8.- S. Gómez-Coca, E. Cremades, N. Aliaga-Alcalde and E. Ruiz, Mononuclear single-molecule magnets: tailoring the magnetic anisotropy of first-row transition-metal complexes, *J. Am. Chem. Soc*., 2013, **135**, 7010-7018.

9.- A. A. Pavlov, D. Y. Aleshin, S. A. Savkina,, A. S. Belov, N. N. Efimov, J. Nehrkorn, M. Ozerov, Y. Z. Voloshin, Y. V. Nelyubina and V. V. Novikov, A trigonal prismatic cobalt(II) complex as a single molecule magnet with a reduced contribution from quantum tunnelling, *ChemPhysChem,* 2019, **20**, 1001-1005.

10.- Y. Peng, T. Bodenstein, K. Fink, V. Mereacre, C. E. Anson and A. K. Powell, Magnetic anisotropy of a Co^{II} single ion magnet with distorted trigonal prismatic coordination: theory and experiment, *Phys. Chem. Chem. Phys.,* 2016, **18**, 30135-30143.

11.- T. J. Ozumerzifon, I. Bhowmick, W. C. Spaller, A. K. Rappé and M. P. Shores, Toward steric control of guest binding modality: a cationic Co(II) complex exhibiting cation binding and zero-field relaxation, *Chem. Commun.,* 2017, **53**, 4211-4214.

12.- M. R. Saber, M. K. Singh and K. R. Dunbar, Geometrical control of the magnetic anisotropy in six coordinate cobalt complexes, *Chem. Commun.,* 2020, **56**, 8492.

13.- A. A. Pavlov, S. A. Savkina, A. S. Belov, Y. V. Nelyubina, N. N. Efimov, Y. Z. Voloshin, V. V. Novikov, Trigonal Prismatic Tris-pyridineoximate Transition Metal Complexes: A Cobalt(II) Compound with High Magnetic Anisotropy, *Inorg. Chem*. 2017, **56**, 6943−6951.

14.- Y. Y. Zhu, C. Cui, Y. Q. Zhang, J. H. Jia, X. Guo, C. Gao, K. Qian, S. D. Jiang, B. W. Wang, Z. M. Wang and S. Gao, Zero-field slow magnetic relaxation from single Co(II) ion: a transition metal single-molecule magnet with high anisotropy barrier, *Chem. Sci.,* 2013, **4**, 1802-1806.

15.- A. Landart-Gereka, M. M. Quesada-Moreno, I. F. Díaz-Ortega, H. Nojiri, M. Ozerov, J. Krzystek, M. A. Palacios and E. Colacio, *Inorg. Chem. Front.*, 2022, **9**, 2810.

16.- .- A. Landart, M.M. Quesada-Moreno, M. A. Palacios, Y. Li, M. Ozerov, J. Krzystek, E. Colacio, Control of the geometry and anisotropy driven by the combination of steric and anion coordination effects in CoII complexes with N6-tripodal ligands: the impact of the size of the ligand on the magnetization relaxation time, *Dalton Trans.*, 2024,**53**, 12876-12892.

17.- E. Zahradníková, R. Herchel, I. Šalitroš, I. Císařová, B. Drahoš, Late first-row transition metal complexes of a 17-membered piperazine-based macrocyclic ligand: structures and magnetism, *Dalton Trans*., 2020,**49**, 9057-9069.

18.- Y. P. Tupolova, I. N. Shcherbakov, L. D. Popov, V. E. Lebedev, V. V. Tkachev, K. V. Zakharov, A. N. Vasiliev, D. V. Korchagin, A. V. Palii, S. M. Aldoshin, Field-induced single-ion magnet behaviour of a hexacoordinated Co(ii) complex with easy-axis-type magnetic anisotropy, *Dalton Trans.,* 2019,**48**, 6960-6970.

19. I. Nemec, O. F. Fellner, Idruchová, R. Herchel, Trigonally Distorted Hexacoordinated Co(II Single-Ion Magnets, *Materials* 2022, **15**, 104.

20.- K. Kotrle, I. Nemec, P. Antal, K. Petrželová, E. Čižmár, Radovan Herchel, 2-Formylphenoxyacetic acid Schiff bases: a promising ligand scaffold for readily available trigonal prismatic Co(ii) single-ion magnets, *Inorg. Chem. Front.*, 2023,**10**, 7319-7332.

21.- . Peng, Y.-B. Peng, G.-X. Zhou, R.-Y. Zhang, Y.-Z. Ma, S. Luo, X.-M. Ren, The Impact of Coordination Distortion on Magnetic Properties of Co (II) Single-Ion Magnets With Trigonal Prism Coordination Geometry, *Applied Organometallic Chemistry* 2025, **39(3)**, e7878.

Table S15. Spin Free CASSCF and CASSCF/NEVPT2 energies (δE, cm^{-1}) for **1**.

States	**1**	
	CASSCF	**NEVPT2**
1	0.0	0.0
2	0.2	0.2
3	4729.0	6019.8
4	6598.4	8831.4
5	6598.7	8832.4
6	6895.5	9394.5

Table S16. Energy levels after the inclusion of spin-orbit effects from CASSCF and CASSCF/NEVPT2 calculations (ΔE, cm^{-1}) for **1**.

States	**1**	
	CASSCF	**NEVPT2**
1	0.00	0.00
2	285.39	292.96
3	610.55	618.79
4	971.38	972.46
5	5035.00	6367.87
6	5174.36	6478.65
7	6916.19	9128.54
8	7049.18	9261.43

Table S17. The ligand field one electron eigenfunctions from CASSCF/NEVPT2 calculations for **1**.

Orbital	**Energy (eV)**	**Energy (cm^{-1})**	d_{z^2}	d_{xz}	d_{yz}	$d_{x^2-y^2}$	d_{xy}
1	0.000	0.0	0.999138	0.007487	-0.040816	-0.000604	-0.000156
2	0.127	1026.6	-0.008885	-0.054646	-0.212834	-0.887499	-0.404948
3	0.127	1026.9	-0.003802	0.257072	-0.043271	-0.405229	0.876251
4	0.941	7586.1	-0.036931	-0.224462	-0.948467	0.192436	0.107849
5	0.941	7586.2	-0.016283	0.938344	-0.227098	0.105371	-0.237844

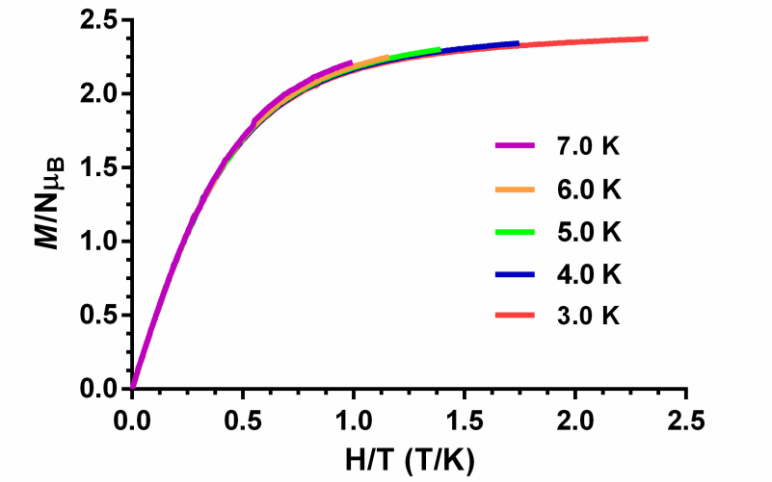

Figure S11.- M vs H/T plot for **1**.

Table S18. Spin Free CASSCF and CASSCF/NEVPT2 energies (δE, cm^{-1}) for **Co-1** and **Co-2 in complex 2'**. **Co-1** and **Co-2** refer to the edge and middle Co(II) ions, respectively.

States	**Co-1**		**Co-2**	
	CASSCF	**NEVPT2**	**CASSCF**	**NEVPT2**
1	0.0	0.0	0.0	0.0
2	102.3	133.5	160.9	222.6
3	4756.5	6134.4	1697.1	2088.8
4	6015.1	7917.5	6756.1	8724.3
5	6116.1	8065.1	6784.3	8800.1
6	6817.4	9126.4	7073.8	9062.9

Table S19. Energy levels after the inclusion of spin-orbit effects from CASSCF and CASSCF/NEVPT2 calculations (ΔE, cm^{-1}) for **Co-1** and **Co-2 in complex 2'**. **Co-1** and **Co-2** refer to the edge and middle Co^{II} ions, respectively.

States	**Co-1**		**Co-2**	
	CASSCF	**NEVPT2**	**CASSCF**	**NEVPT2**
1	0.00	0.00	0.00	0.00
2	277.79	282.53	239.86	233.11
3	618.31	634.67	567.61	596.34
4	976.12	982.34	906.31	914.40
5	4995.45	6399.44	2071.96	2430.90
6	5126.68	6507.29	2178.08	2526.88
7	6336.44	8221.92	7093.68	9021.31
8	6480.76	8354.18	7168.47	9090.17

Table S20. Contributions to *D*-tensor of **Co-1** and **Co-2** from CASSCF/NEVPT2 calculations.

	Co-1		**Co-2**	
	D	*E*	*D*	*E*
$^4\Phi_1$	-161.052	-0.001	-134.942	-0.005
$^4\Phi_2$	3.787	-3.771	13.435	-13.478
$^4\Phi_3$	4.129	-1.260	0.046	0.046
$^4\Phi_4$	4.509	1.688	0.622	-3.864
$^4\Phi_5$	2.337	2.309	6.413	6.413

Table S21. The ligand field one electron eigenfunctions for **Co-1** and **Co-2** from CASSCF/NEVPT2 calculations.

Co-1

Orbital	**Energy (eV)**	**Energy (cm^{-1})**	d_{z^2}	d_{xz}	d_{yz}	$d_{x^2-y^2}$	d_{xy}
1	0.000	0.0	-0.999140	-0.018732	-0.001924	0.019529	-0.031351
2	0.224	1809.5	-0.021779	0.258065	-0.084961	0.471391	0.838749
3	0.243	1962.8	-0.028761	-0.099424	-0.263721	-0.834699	0.472245
4	0.895	7221.8	0.018180	-0.950287	-0.137394	0.238085	0.145130
5	0.910	7338.2	0.009317	0.141849	-0.950974	0.154925	-0.226801

Co-2

Orbital	**Energy (eV)**	**Energy (cm^{-1})**	d_{z^2}	d_{xz}	d_{yz}	$d_{x^2-y^2}$	d_{xy}
1	0.000	0.0	-0.833706	0.287008	-0.000049	-0.471764	0.000059
2	0.039	311.8	0.545614	0.296498	0.000097	-0.783833	0.000245
3	0.052	420.2	-0.000118	-0.000061	0.511829	0.000227	0.859087
4	0.938	7564.3	-0.000040	0.000006	0.859087	-0.000079	-0.511829
5	1.035	8346.9	0.085089	0.910887	0.000012	0.403788	-0.000038

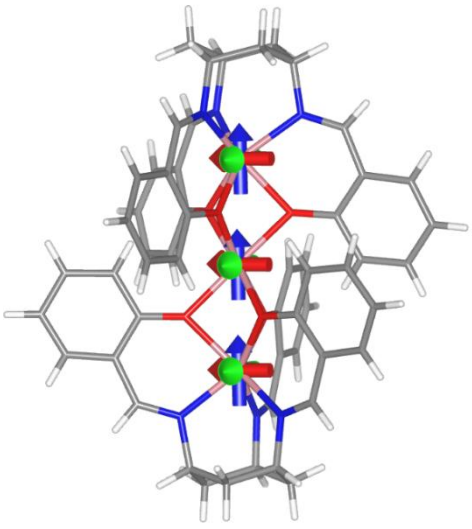

Figure S12. Orientation of the *g*-tensor components in **Co-1** and **Co-2**, obtained from CASSCF/NEVPT2 calculations. The reference axis *x*, *y* and *z* of the *g*-tensor are displayed in red, green and blue, respectively. Counterions and solvent molecules have been omitted for clarity.

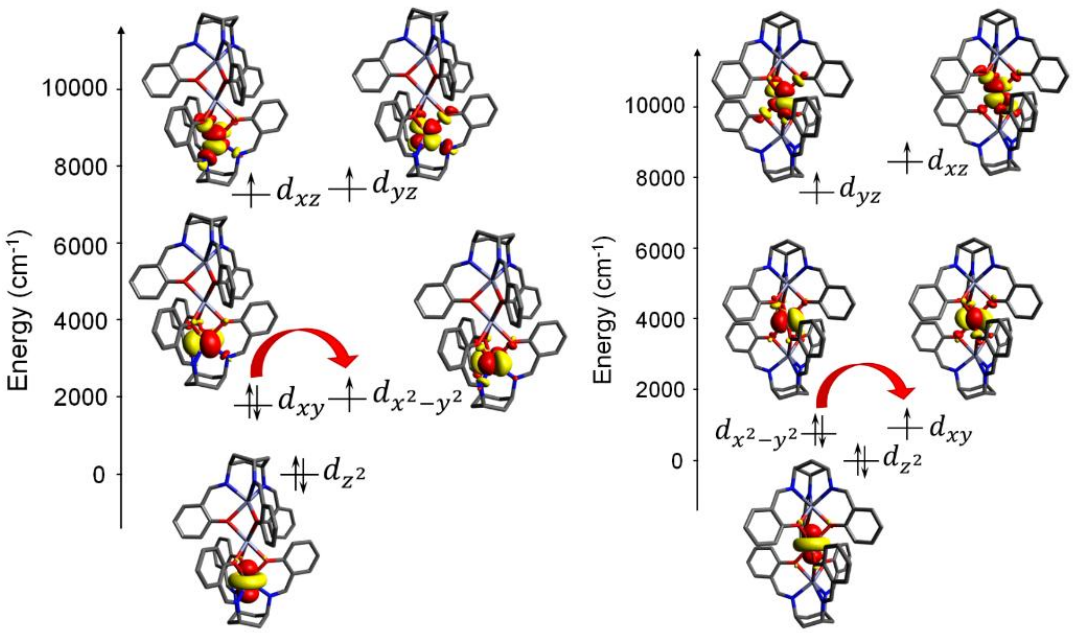

Figure S13. NEVPT2-AILFT computed d-orbital energy diagram of **Co-1** (left) and **Co-2** (right) of complex **2'**. Hydrogen atoms are omitted for clarity.

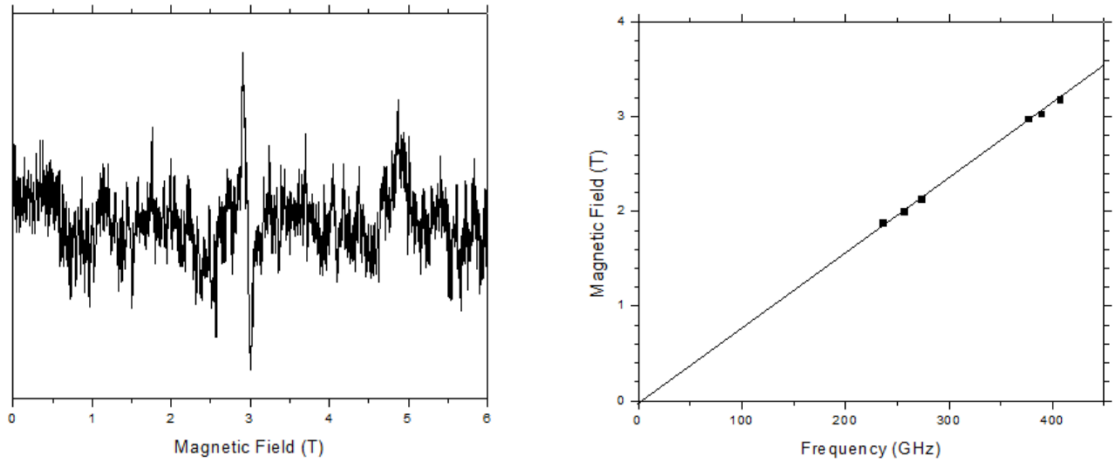

Figure S14. (Left) An HFEPR spectrum of **1** at 4.5 K and 378 GHz. The resonance appears at almost exactly 3 T. (Right) A field vs. frequency plot of the resonance as in Figure 1 at 4.5 K. The line represents a *g*-value of 9.08.

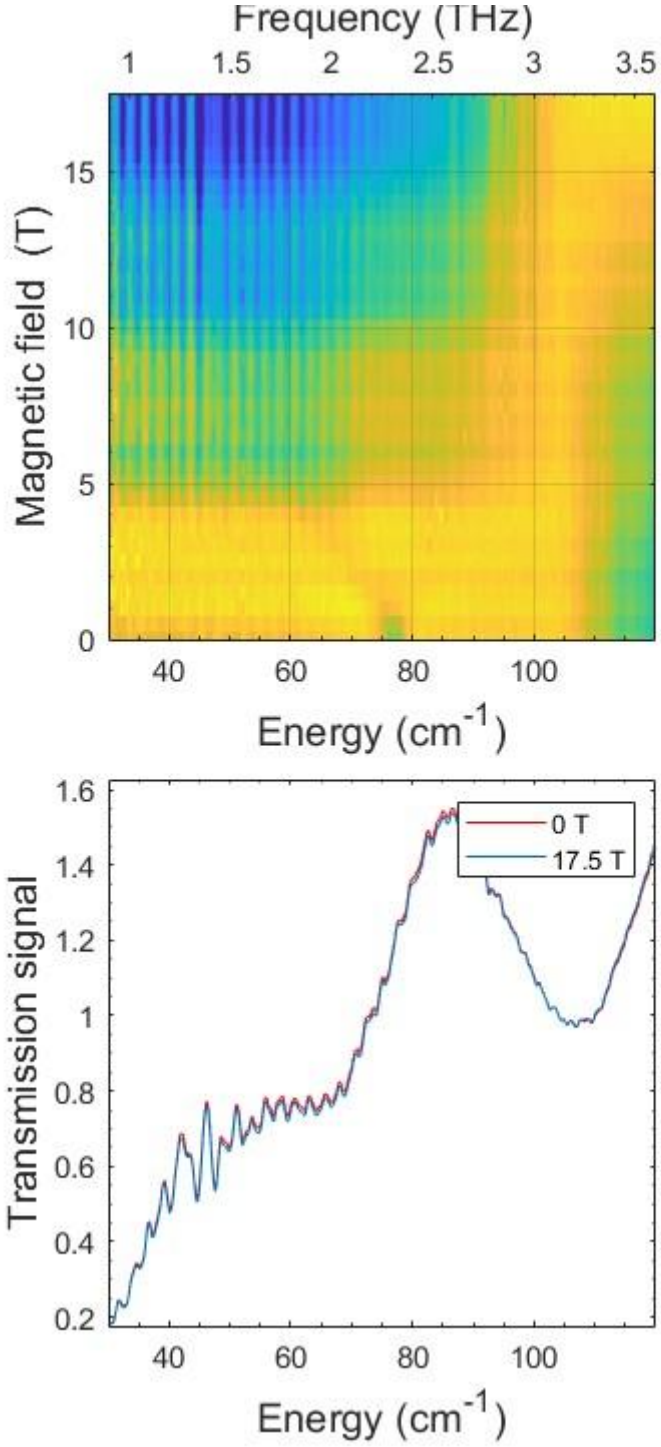

Figure S15.- (Top) Experimental 2-D (magnetic field vs. energy) heat maps of FIRMS response of complex **2'**. Regions marked in blue represent resonance absorption that is sensitive to changing magnetic field. Regions in yellow are insensitive to the field. The most intense change is observed at 76.8 cm^{-1} in zero field. (Right) Transmission spectra recorded on powder pellet of the complex at T = 4.2 K and at the indicated magnetic fields.

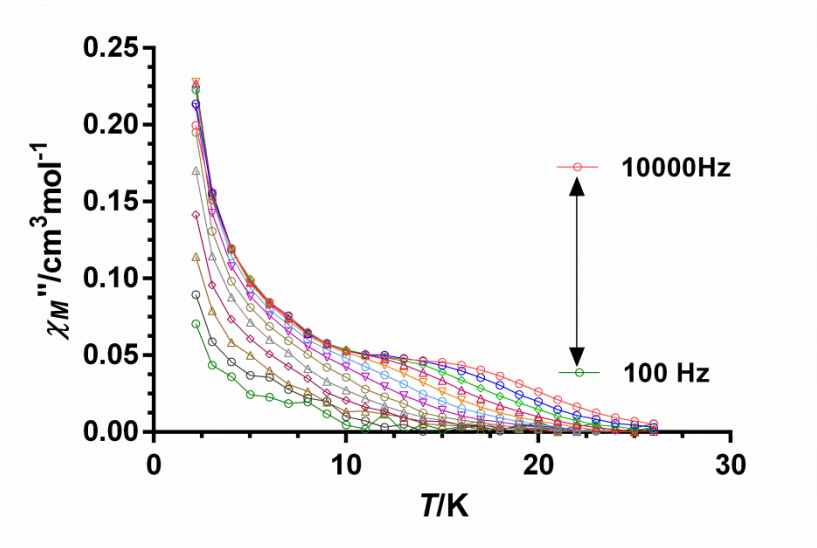

Figure S16.- Temperature dependence of χ''_M for **1** at different frequencies under zero applied magnetic field.

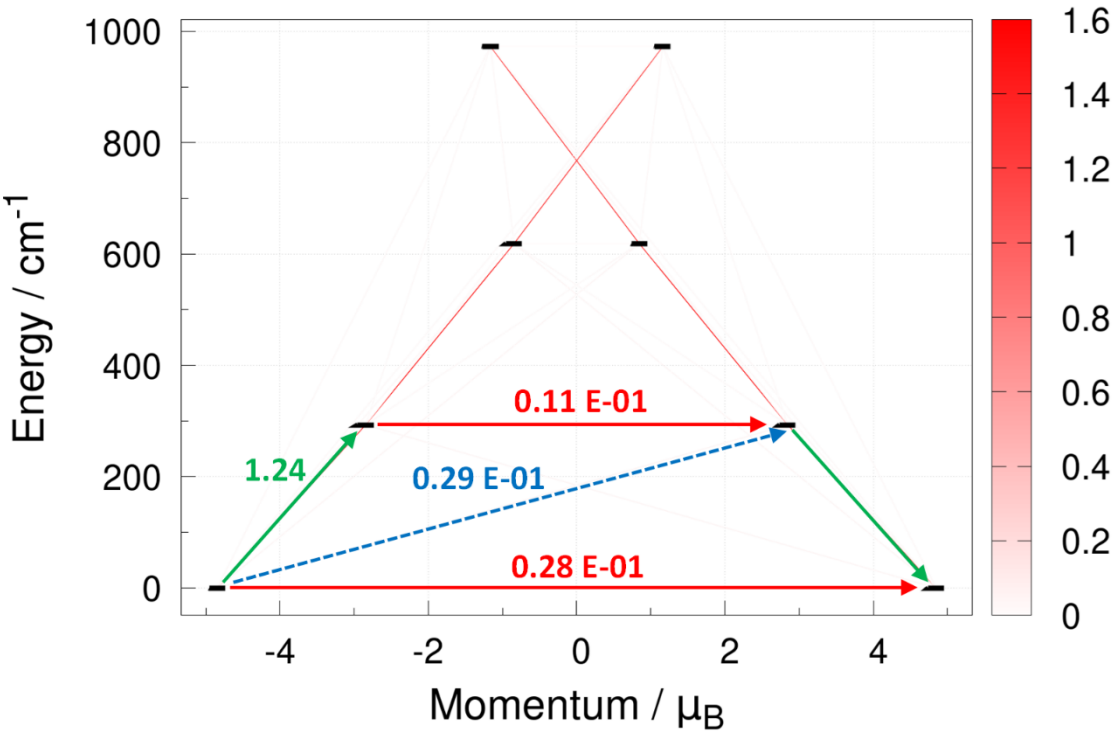

Figure S17. *Ab initio* calculated relaxation pathways in compound **1**. The black lines indicate the KDs as a function of the magnetic moments. Red lines denote QTM in the ground state and TA/QTM through the first and second excited states. Blue dashed lines represent possible Orbach processes.

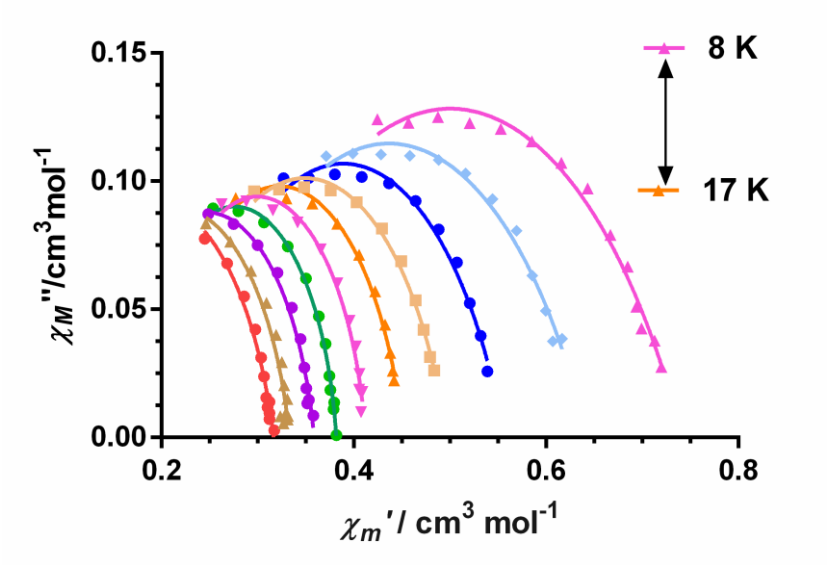

Figure S18.- Cole-Cole plots for compound **1** at zero dc field in the indicated temperature range.

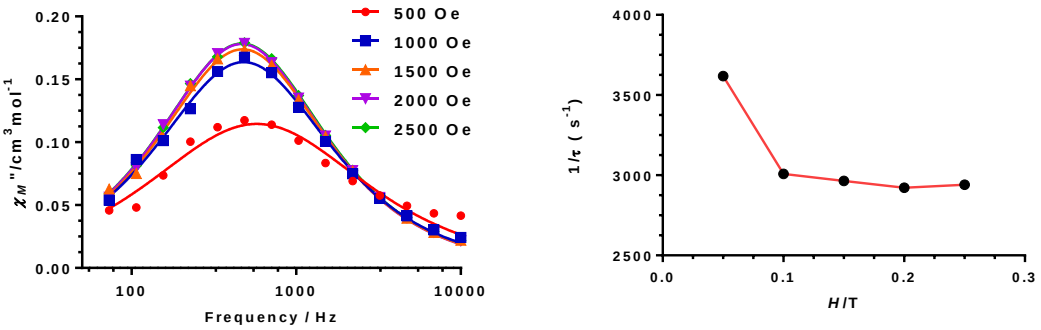

Figure S19.- Frequency dependence of the χ''_M at 10 K at the indicated magnetic fields (left) and field dependence of τ^{-1} (right) for **1**.

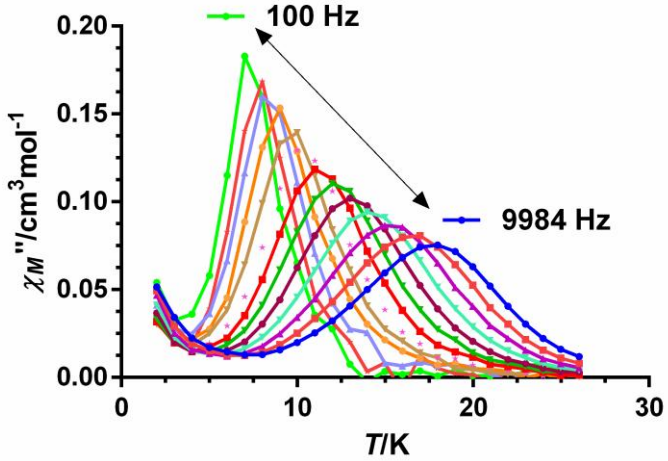

Figure S20.- Temperature dependence of χ''_M for **1** at different frequencies under a H_{dc} = 2000 Oe.

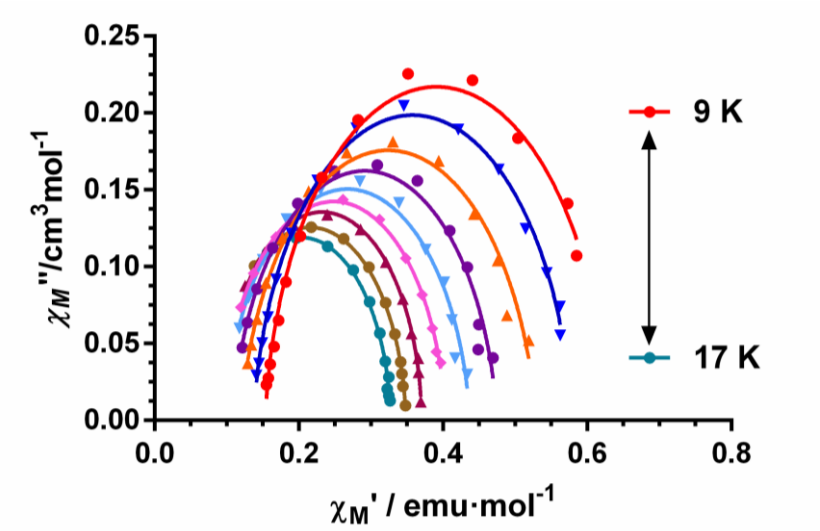

Figure S21.- Cole-Cole plots for compound **1** at H_{dc} = 2000 Oe in the indicated temperature range.

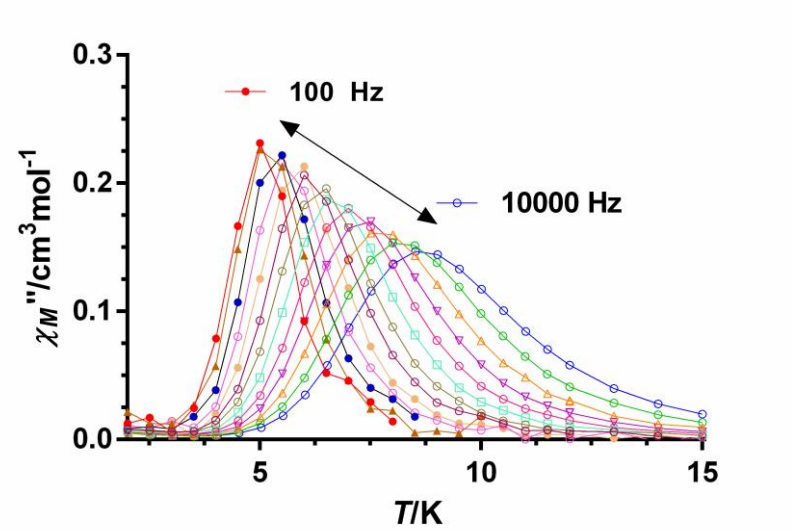

Figure S22.- Temperature dependence of χ''_M for **2'** at zero dc field in the indicated frequencies range.

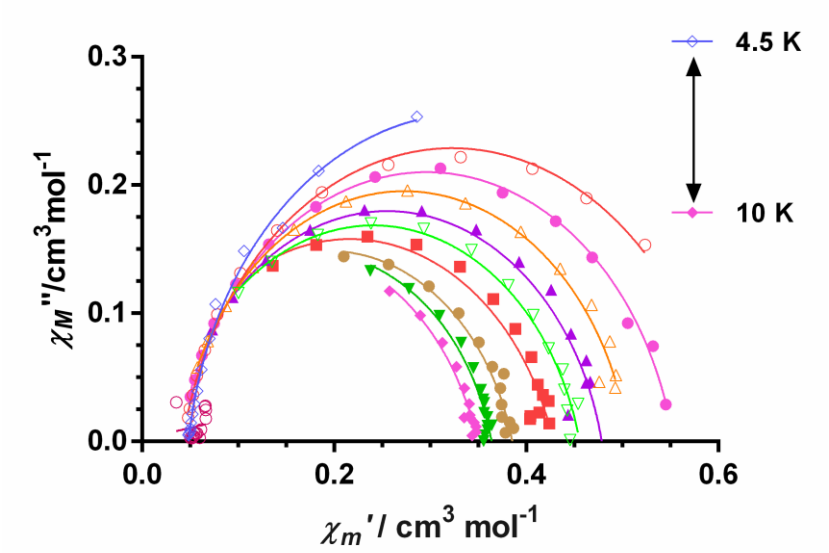

Figure S23.- Cole-Cole plots for compound **2'** at zero field in the indicated temperature range.

Co-1

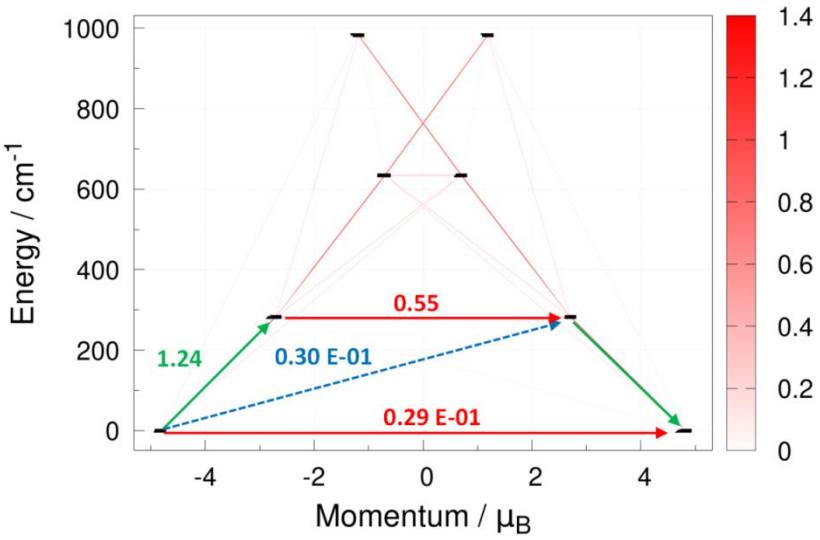

Co-2

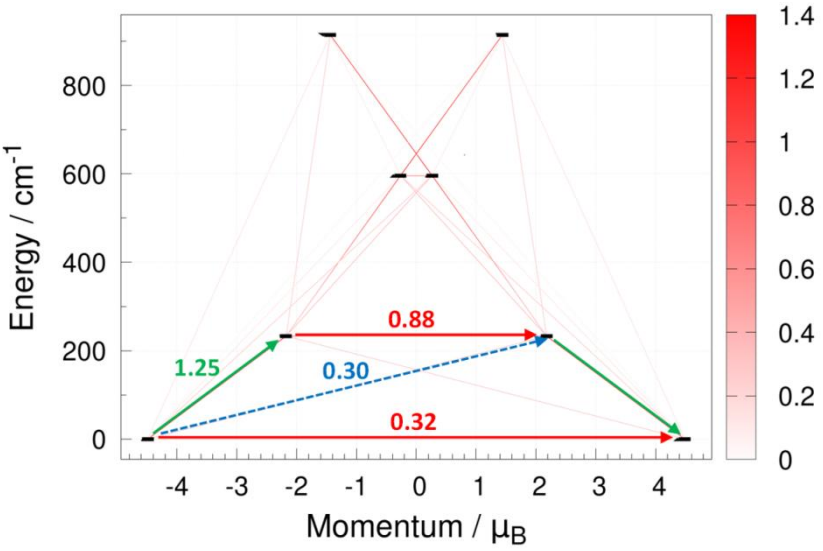

Figure S24. *Ab initio* calculated relaxation pathways in in **Co-1** and **Co-2** of compound **2'**. The black lines indicate the KDs as a function of the magnetic moments. Red lines denote QTM in the ground state and TA/QTM through the first and second excited states. Blue dashed lines represent possible Orbach processes.

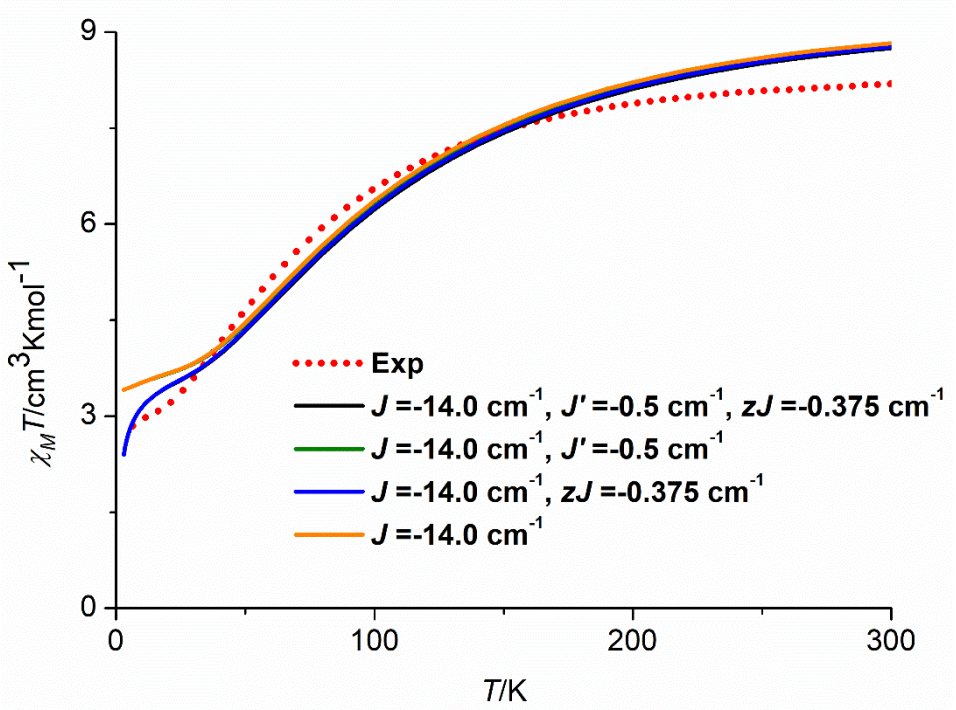

Figure S25. Temperature dependence of the $\chi_M T$ product for **2'** (red circles) and POLY_ANISO fits with the indicated parameters (solid lines in different colours).